

# On the Nature of the ‘Quasiparticle’ Peak in the Angular Resolved Spectrum of the Superconducting Underdoped $\text{Bi}_2\text{Sr}_2\text{CaCu}_2\text{O}_8$ .

A.V. Rozhkov

*Center for Materials Theory, Department of Physics and Astronomy, Rutgers University,  
136 Frelinghuysen Road, Piscataway, NJ 08854, USA*

## Abstract

We study the reconfiguration of the angular resolved photoemission spectrum near  $M$  point which occurs in  $\text{Bi}_2\text{Sr}_2\text{CaCu}_2\text{O}_8$  upon cooling below the superconducting transition temperature. Restricting our attention to the case of underdoped samples we offer a phenomenological mechanism-independent argument which explains the emergence of a peak in the spectrum in terms of the normal state pseudogap. All of the basic experimental observations, including the peak dispersion, ‘dip-and-hump’ shape of the superconducting state spectrum and appearance of the peak at the temperatures somewhat higher than  $T_c$ , are naturally explained.

## I. INTRODUCTION

A sharp peak in the angular resolved photoemission spectrum of  $\text{Bi}_2\text{Sr}_2\text{CaCu}_2\text{O}_8$  (BSCCO) is the major subject of this paper [1–3]. This peak emerges from an incoherent background at temperatures somewhat higher than  $T_c$  and persists all the way down to  $T = 0$ . It is located around  $(\pi, 0)$  (in the units of inverse lattice spacing) in the Brillouin zone. Substantial efforts have been invested into uncovering the nature of this peak. It was assumed that this might provide us with an important clue about a mechanism of the superconducting state. In this paper we will argue that the peak is a consequence of normal state phenomenology. Our method will enable us to explain qualitatively the most salient features of the peak behavior.

Unlike overdoped cuprates, it is believed that for the underdoped materials the normal state single-particle Green’s function can be qualitatively characterized by the presence of the pseudogap – a depletion of the spectral density  $A_{n\mathbf{k}}(\omega) = -2\text{Im} G_{n\mathbf{k}}(\omega)$  near  $\omega = 0$  for  $\mathbf{k}$  in the vicinity of  $M$  point of the Brillouin zone close to the Fermi surface (see fig.1b). The origin of the pseudogap is unclear at the moment. Yet, our method does not require such knowledge.

The causality puts some constraints on the Green’s function: its real part can be found according to the Kramers transformation [5]. Then, for any reasonable choice of “pseudogapped”  $A_{n\mathbf{k}}(\omega)$  the function  $|\text{Re}G_{n\mathbf{k}}(\omega)|$  has two maxima located approximately at the

edges of the pseudogap (fig.1a). We will show that those maxima are responsible for the emergence of the ‘quasiparticles’ in the superconducting state.

There are several microscopical theories which explain the emergence of the peak below  $T_c$  [6–8]. In the approach presented by J.E. Hirsch charge carriers (holes) are coupled to a bosonic bath. If this coupling weakens with the growth of the local hole concentration the superconducting pairing driven by the kinetic energy occurs: the kinetic energy benefits from the effective reduction of the boson-hole coupling. Another consequence of this boson-hole decoupling is the increase of the quasiparticle peak weight. In the paper by M. Eschrig *et al.* a model of the electrons interacting with a magnetic resonance has been discussed. It is claimed that this model reproduces correctly the most salient features of the photoemission spectrum. This paper was a development of a previous work by M. Norman, H. Ding and collaborators [9,10]. The latter is important to us since it has some similarities with the present approach. In Ref. [9,10] the authors concentrated their attention on a step-like feature in the electron self-energy which could explain the shape of the spectrum. In order to account for such a feature they postulated the existence of a collective mode below  $T_c$ . This mode has to disappear above  $T_c$  for the model predictions to be consistent with the data. It is believed that this mode and the magnetic resonance mentioned above are the same entity. Many-body investigation of the phenomenon was undertaken by E. Carlson *et al.* They assume that in the cuprate materials phase separation takes place. It leads to the formation of stripes with every stripe being 1D metallic conductor. Using bosonization the authors demonstrated that below  $T_c$  the single-particle spectral density develops a delta-function peak at the superconducting gap energy.

In contrast to these studies, we will deduce this peak without resorting to microscopical considerations. It will be shown that the peak in the single-particle spectral density is a consequence of the analytical structure of the normal state Green’s function.

## II. ANALYTICAL STRUCTURE OF THE SINGLE ELECTRON PROPAGATOR

In this part of the paper we will calculate the spectral density in the superconducting state. Let us derive first an auxiliary relation between the Green’s function of an electron and a hole. The spin-up electron retarded propagator is:  $G^e(t) = -i\Theta(t)\langle c_\uparrow(t)c_\uparrow^\dagger(0) + c_\uparrow^\dagger(0)c_\uparrow(t) \rangle$ . The propagator for a spin-up hole:

$$G^h(t) = -i\Theta(t)\langle c_\downarrow^\dagger(t)c_\downarrow(0) + c_\downarrow(0)c_\downarrow^\dagger(t) \rangle = \left( i\Theta(t)\langle c_\downarrow^\dagger(0)c_\downarrow(t) + c_\downarrow(t)c_\downarrow^\dagger(0) \rangle \right)^* = \left( i\Theta(t)\langle U_x^{-1}c_\downarrow^\dagger(0)U_xU_x^{-1}c_\downarrow(t)U_x + U_x^{-1}c_\downarrow(t)U_xU_x^{-1}c_\downarrow^\dagger(0)U_x \rangle \right)^* = (-G^e(t))^*. \quad (1)$$

Here  $U_x$  is the unitary rotation operator. It rotates the spin of the electron by  $\pi$  around  $x$  axis:  $U_x^{-1}c_\alpha U_x = i\sigma_{\alpha\beta}^x c_\beta$  and  $U_x^{-1}c_\alpha^\dagger U_x = -i\sigma_{\alpha\beta}^x c_\beta^\dagger$ . The ground state is invariant under the action of  $U_x$ . After performing Fourier transformation for the last equality one arrives at:

$$G^h(\omega) = -(G^e(-\omega))^*. \quad (2)$$

Assume now that the system at hand is in the normal state but not far from the superconducting transition. Its retarded Green’s function in Nambu representation can be written as:

$$\hat{G}_{n\mathbf{k}}(\omega) = \begin{pmatrix} G_{n\mathbf{k}}(\omega) & 0 \\ 0 & -G_{n-\mathbf{k}}^*(-\omega) \end{pmatrix} = \begin{pmatrix} G_{n\mathbf{k}}(\omega) & 0 \\ 0 & -G_{n\mathbf{k}}^*(-\omega) \end{pmatrix} \quad (3)$$

In this form it describes independent propagation of an electron and a hole. Spatial inversion symmetry guarantees that  $G_{-\mathbf{k}} = G_{\mathbf{k}}$ .

This function  $\hat{G}_n$  satisfies Dyson's equation:

$$(\omega - \mathcal{H}_0)\hat{G}_{n\mathbf{k}}(\omega) = \hat{1} + \hat{\Sigma}_{n\mathbf{k}}(\omega)\hat{G}_{n\mathbf{k}}(\omega). \quad (4)$$

Here  $\hat{\Sigma}_n$  is the retarded self-energy in the normal state:

$$\hat{\Sigma}_{n\mathbf{k}}(\omega) = \begin{pmatrix} \Sigma_{n\mathbf{k}}(\omega) & 0 \\ 0 & -\Sigma_{n\mathbf{k}}^*(-\omega) \end{pmatrix}. \quad (5)$$

Next, we change, let's say, doping and drive the system superconducting. New Green's function  $\hat{G}_s$  satisfies an equation similar to (4) with new self-energy  $\hat{\Sigma}_{s\mathbf{k}} = \hat{\Sigma}_{n\mathbf{k}} + \hat{\sigma}_{\mathbf{k}}$  where  $\hat{\sigma}$  given by:

$$\hat{\sigma}_{\mathbf{k}}(\omega) = \begin{pmatrix} \mu_{\mathbf{k}}(\omega) & \sigma_{\mathbf{k}}^A(\omega) \\ (\sigma_{\mathbf{k}}^A(-\omega))^* & -(\mu_{\mathbf{k}}(-\omega))^* \end{pmatrix}. \quad (6)$$

Here the relation  $\Sigma_{12}(\omega) = (\Sigma_{21}(-\omega))^*$  between two off-diagonal elements of the Nambu self-energy has been used. It follows from an equation  $G_{12}(\omega) = G_{21}^*(-\omega)$  for anomalous propagators which, in turn, can be obtained along the same lines as (2). The point of this derivation is to establish the analytical structure of the self-energy in the superconducting state. This will be used in our discussion of a sum rule.

Combining the above equations one gets for  $\hat{G}_s$  the expression:

$$\hat{G}_{s\mathbf{k}} = \left( \hat{G}_{n\mathbf{k}}^{-1} - \hat{\sigma}_{\mathbf{k}} \right)^{-1}. \quad (7)$$

### III. GREEN'S FUNCTION IN THE SUPERCONDUCTING STATE

The equations derived in the previous section are completely general. In order to proceed further we need to make a simplifying assumption: near the Fermi surface electronic ( $\omega < 0$ ) and hole ( $\omega > 0$ ) parts of the spectral function are symmetric for small  $|\omega|$ . One can express that as:

$$A_{\mathbf{k}}(\omega) = A_{\mathbf{k}}(-\omega) \quad (8)$$

for  $|\omega| < \omega_g$  where  $\omega_g$  is the size of the pseudogap. Exact particle-hole symmetry is absent in the cuprates. We would like to argue, however, that (8) holds at least approximately for  $\mathbf{k}$  close to the Fermi surface. Firstly, the tunneling data [11] shows that the pseudogap is symmetric with respect to voltage polarity change. One might think that this tells little about validity of (8) since the tunneling differential conductance measures  $\mathbf{k}$ -integrated spectral density. However, Ding *et al.* (inset of fig.1b of Ref. [2]) demonstrated that scanning tunneling microscope (STM) spectrum multiplied by the Fermi distribution function at appropriate temperature coincides with the angular-resolved spectral density at  $\mathbf{k} = (\pi, 0)$ .

This means that STM spectrum equal to  $A_{\mathbf{k}}(\omega)$  for  $\omega < 0$ . It is natural to expect that the spectral density coincide with the STM conductivity for  $\omega > 0$  as well. Thus, the symmetry of the STM data suggests the symmetry of the photoemission spectrum. Although, it is not our goal to construct a theory of tunneling into cuprates we may speculate that this agreement between the tunneling conductance and the photoemission spectrum is not a coincidence but a consequence of the inter-plane hopping matrix element  $\mathbf{k}$ -dependence: as discussed before [12–14] the inter-plane hopping matrix element is at its maximum for the electrons with a momentum parallel to  $(\pi, 0)$  and it vanishes along Brillouin zone diagonal. Therefore, it is conceivable that the most of the tunneling current is carried by the electrons near  $(\pi, 0)$ . Secondly, we would like to direct our attention toward the discussion of Ref. [15]. In the latter paper the angular resolved spectrum at  $\mathbf{k} = \mathbf{k}_F$  was analyzed with the help of a momentum distribution sum rule. Theoretically, it was proved that an expression  $1 - \int_0^\infty d\omega \tanh(\omega/2T)(A_{\mathbf{k}_F}(\omega) - A_{\mathbf{k}_F}(-\omega))$  has to be temperature independent provided that (8) is true for small  $|\omega|$  [16]. This expression can be easily extracted from the data since it is proportional to the integral over  $\omega$  of the photoemission spectrum. The spectrum for  $\mathbf{k}$  near  $(\pi, 0)$  was integrated, and the integral showed no dependence on the temperature, supporting the assumption of the symmetry. Finally, we would like to mention two other papers [17,18] where (8) was assumed to be true. Thus, we believe we have enough evidence to treat (8) as a reasonable approximation for small  $|\omega|$ . The structure of the background for  $|\omega| > \omega_g$  is of little interest to us since the positions of  $|\text{Re } G_n|$  maxima are insensitive to the background. For the purpose of simplicity we will assume that the background is also symmetric. That is, (8) is true for any  $\omega$ . In such a case Green's function satisfies  $G_{\mathbf{k}}(-\omega) = -G_{\mathbf{k}}^*(\omega)$ .

A consequence of the symmetry is a constraint on the self-energy in the superconducting phase:

$$\hat{\sigma}_{\mathbf{k}}(\omega) = \begin{pmatrix} \mu_{\mathbf{k}}(\omega) & \sigma_{\mathbf{k}}^A(\omega)e^{i\phi} \\ \sigma_{\mathbf{k}}^A(\omega)e^{-i\phi} & \mu_{\mathbf{k}}(\omega) \end{pmatrix}, \quad (9)$$

where  $\phi$  is a real number and the functions  $\mu$  and  $\sigma^A$  satisfy the following:

$$\mu_{\mathbf{k}}(-\omega) = -\mu_{\mathbf{k}}^*(\omega) \quad \text{and} \quad \sigma_{\mathbf{k}}^A(-\omega) = (\sigma_{\mathbf{k}}^A(\omega))^*. \quad (10)$$

In terms of these functions the superconducting spectral density equals to:

$$A_{s\mathbf{k}} = -2\text{Im} \left\{ \frac{G_{n\mathbf{k}} - (G_{n\mathbf{k}})^2 \mu_{\mathbf{k}}}{(1 - G_{n\mathbf{k}}\mu_{\mathbf{k}})^2 - (\sigma_{\mathbf{k}}^A)^2 (G_{n\mathbf{k}})^2} \right\}. \quad (11)$$

Let us simplify this equation. If the system is close to the transition point then  $\hat{\sigma}$  is small and the denominator of (11) is close to unity everywhere except the edges of the pseudogap. At those points as one can see from fig.1a  $(\text{Re } G_n)^2$  is big and one should be more careful. If we are away from the Brillouin zone diagonal where  $\sigma^A$  is zero then to the second order in  $\sigma^A$  and to the first order in  $\mu = \mathcal{O}(|\sigma^A|^2)$  we find that the denominator is equal to  $1 - (\sigma^A)^2 (G_n)^2$ . In this expression the terms like  $G_n \mu$  have been dropped. Although, they are of the order of  $|\sigma^A|^2$  we presume that they are smaller than  $(\text{Re } G_n)^2 |\sigma^A|^2$  since the latter is proportional to the second power of  $\text{Re } G_n$  which is big at the pseudogap edges. This gives for the spectral function:

$$A_{s\mathbf{k}}(\omega) \simeq \frac{A_{n\mathbf{k}}(\omega)}{1 - \text{Re} \left\{ (\sigma_{\mathbf{k}}^{\mathcal{A}}(\omega))^2 \right\} (\text{Re } G_{n\mathbf{k}}(\omega))^2}, \quad (12)$$

where we omit  $(G_n)^2 \mu$  term in the numerator assuming that it is small compare to  $G_n$ . The last formula is the key to understanding the appearance of the ‘quasiparticles’ below  $T_c$ . At the edges of the pseudogap  $(\text{Re } G_n)^2$  peaks up, the denominator gets smaller and the spectral function develops a sharp maximum. This is true provided that  $\text{Re} \left\{ (\sigma^{\mathcal{A}})^2 \right\}$  is positive at the edges of the pseudogap [19].

#### IV. SPECTRUM PROPERTIES

Now we would like to analyze (11) and (12) to obtain simple properties of the ‘quasiparticles’ which can be compared against the experiment.

First, it is clear that the position of the peak in the frequency domain is determined by the pseudogap edge. Therefore, we expect to see strong correlation between the size of the pseudogap and the frequency (binding energy) position of the peak. This is precisely the effect reported in [1] where temperature dependence of the peak frequency was compared against that of the pseudogap size. Fig.2C of that paper shows that the peak position traces the size of the pseudogap. Similar phenomena is seen for the peak dispersion (binding energy vs.  $\mathbf{k}$ ). As reported in [20] the pseudogap at  $(\pi, 0)$  is virtually  $\mathbf{k}$ -independent. This is consistent with the weak dispersion of the peak itself [21].

In order to obtain the shape of the spectral function at  $\mathbf{k} = (\pi, 0)$  we performed simple numerical study. We modeled  $\mu$ ,  $\sigma^{\mathcal{A}}$  and  $A_n$  as

$$\begin{aligned} \mu &= 0 \\ \text{Re } \sigma_{\mathbf{k}}^{\mathcal{A}} &= \sigma_0^{\mathcal{A}} \exp(-(\omega/\omega^{\mathcal{A}})^2) \end{aligned} \quad (13)$$

$$A_{n\mathbf{k}} = A_0 (\arctan((\omega - \omega_g)/\omega_e) - \arctan((\omega + \omega_g)/\omega_e) + \pi) \exp(-|\omega/W|).$$

The energy  $\omega_e$  determines how abrupt the edges of the pseudogap,  $W$  mimics the bandwidth. The constant  $A_0$  has to be determined from the sum rule [5]:

$$\int_{-\infty}^{+\infty} \frac{d\omega}{2\pi} A_{\mathbf{k}}(\omega) = 1. \quad (14)$$

The parameter  $\omega^{\mathcal{A}}$  describes the frequency dependence of the anomalous self-energy. It is commonly put equal to infinity. This makes the anomalous self-energy frequency independent. Below we will discuss both cases of finite and infinite  $\omega^{\mathcal{A}}$ .

The imaginary part of  $\sigma^{\mathcal{A}}$  and the real part of the Green’s function can be found with the help of numerical Kramers transformation. Then the spectral function in the superconducting state is determined using (11). The resultant spectra for different parameter values are presented on fig.2 and fig.3. These two figures correspond to different values of  $\omega^{\mathcal{A}}$  ( $\omega^{\mathcal{A}}/\omega_g = 15$  for fig.2 and  $\omega^{\mathcal{A}}/\omega_g = 7$  for fig.3). On each figure the top (bottom) row corresponds to  $\sigma^{\mathcal{A}}/\omega_g = 25$  ( $\sigma^{\mathcal{A}}/\omega_g = 15$ ). The value of  $\omega_e/\omega_g$  in the left (right) column is

0.3 (0.1). We see clear ‘dip-and-hump’ structure of the spectrum for big values of  $\sigma^A$ . When this quantity is small we find only a tiny bump or even a kink instead of a well-developed peak. Such situation seems to be realized in Pb-doped BSCO compound [22]. This angular resolved photoemission study revealed no peak in the spectrum (fig.3, right panel of the latter reference). Authors claim that their energy resolution is high enough to observe the peak should it be present in the spectrum.

By comparing different spectra from fig.2 and 3 we can discuss the dependence of the spectrum shape on the model parameters. Two parameters which affect the spectrum the most are  $\sigma^A/\omega_g$  and  $\omega_e/\omega_g$ . The effect of  $\sigma^A$  is obvious: the bigger the anomalous self-energy the higher the peak. The ratio  $\omega_e/\omega_g$  regulates the height of the peaks of  $\text{Re } G_n$ . This height is proportional to  $-\ln(\omega_e/\omega_g)$ . Thus, the smaller this ratio the higher the peak in the superconducting spectrum. The value of  $\omega^A$  specifies roughly the position of the hump. For  $\omega^A = \infty$  the hump is absent from the spectrum – it is moved to infinite frequency.

Another interesting property of our superconducting state spectrum is its compliance with the sum rule (14). Mathematical proof of this fact is given in Appendix. Visually, one can notice from figures 2 and 3 that the depletion of the spectral weight in the dip is roughly compensated by its enhancement at the hump. Experimentally, however, it is seen that the weight from the dip goes into the peak. The reason for this discrepancy is the lack of exact knowledge about  $\hat{\sigma}$ . Particular, we are unable to identify any first principal based constraint which would provide us with any information about  $\mu$ . To keep our consideration as simple as possible we chose to put  $\mu$  equal to zero.

As we stressed the equality (8) is only an approximation. Thus, an interesting question worth discussing is how deviations from (8) affect the peak in the superconducting state. To address this issue we model the electron spectral function as

$$A_{n\mathbf{k}}^e(\omega) = A_{n\mathbf{k}}(\omega + \Delta\omega), \quad (15)$$

where  $A_{n\mathbf{k}}(\omega)$  is given by (13). In this case the pseudogap for electrons is bigger than the pseudogap for holes by the amount of  $2\Delta\omega$ . The spectral function can be found according to

$$A_{s\mathbf{k}}^e = -2\text{Im} \left\{ \frac{G_{n\mathbf{k}}^e}{1 - (\sigma_{\mathbf{k}}^A)^2 G_{n\mathbf{k}}^h G_{n\mathbf{k}}^e} \right\}. \quad (16)$$

The resulting function for  $\Delta\omega = 0.2\omega_g$  and  $\sigma^A(\omega) \equiv 25\omega_g$  is plotted on fig.4. As one can see the only effect of the asymmetry is uneven height of the peaks for positive and negative frequencies. The reason for this becomes clear if one notices that (16) may be approximated in the manner similar to (12):

$$A_{s\mathbf{k}}^e \simeq \frac{A_{n\mathbf{k}}^e}{1 - (\sigma_{\mathbf{k}}^A)^2 \text{Re} \left\{ G_{n\mathbf{k}}^h G_{n\mathbf{k}}^e \right\}}. \quad (17)$$

In order to demonstrate the quality of this approximation we plotted this expression on fig.4. The denominator in (17) is symmetric with respect to the frequency sign change. It has two minima located approximately at  $\pm\omega_g$ . Since  $A_n^e(\omega_g) > A_n^e(-\omega_g)$  the peak at  $\omega < 0$  is smaller. It is now clear that the superconducting state spectrum is rather robust with respect to small deviations from (8).

To understand why the peak appears at the temperatures higher than  $T_c$  it is enough to imagine that in the cuprates there is a temperature window  $T_{\text{local}} > T > T_c$  where the phase coherence exists over some finite time scale  $\tau(T)$ ,  $\tau \rightarrow \infty$  as  $T \rightarrow T_c$ . Experimental evidence of this was produced by [23]. Speaking more technically, in this temperature window one can use (9) with non-zero  $\sigma^A$  and fixed  $\phi$  to describe the single-particle dynamics on the time scale less than  $\tau$ . For time periods bigger than  $\tau$  the dynamics of the phase  $\phi$  cannot be neglected anymore. If  $\tau$  is big enough one can simply average the propagator over the phase fluctuations. For infinitely long time the anomalous propagator always vanishes above  $T_c$  due to the phase dynamics. However, the peak in the photoemission spectrum does not vanish since, as it follows from (11), it is independent of  $\phi$ .

## V. DISCUSSION

We study the ‘quasiparticle’ peak in the superconducting state of the underdoped BSCCO. The main conclusion of the present work is that the peak can be explained on the basis of the normal state phenomenology. Our analysis is based on three premises. First, we assume that the single particle spectrum has a pseudogap (fig.1b). The most important consequence of that is the peaks of the function  $|\text{Re } G_n(\omega)|$  at the edges of the pseudogap. Next, we assume that there is approximate symmetry between positive-frequency and negative-frequency parts of the spectrum (8). This guarantees that the function  $-\text{Re } \{G_n(\omega)G_n(-\omega)\}$  has only one maximum at  $\omega < 0$ . We also shown that some violation of (8) is not fatal for the qualitative structure of the superconducting state spectrum. Finally, there is the third assumption we made implicitly: the single-particle anomalous self-energy  $\sigma^A(\omega)$  does not go to zero at the edges of the pseudogap. If  $\sigma^A$  does go to zero then the peak in the superconducting phase could be completely suppressed (see (12)).

In order to explain the emergence of the peak at  $T > T_c$  we accepted another postulate. It was agreed that (9) local order parameter is established and it is permissible to use (9) with fluctuating  $\phi$  to describe the single-particle dynamics above  $T_c$ .

The fact that the peak can be derived from the normal state properties suggests that it is not a fundamental object. Moreover, depending on the circumstances it may be absent or replaced by a less prominent feature [22].

It is also can be surmised that this phenomena may not be limited to the cuprate superconductors only. The peak could be present in the superconducting state of any material which has a pseudogap in the normal state.

We did not try to fit any experimental data by our curves from fig.2 and fig.3. It is not possible owing to the lack of knowledge about exact form of functions (13). We also have no independent information about the values of  $\omega_e$ ,  $\omega^A$ ,  $\sigma_0^A$ . Another argument against feasibility of the spectrum fit is a problem with the experimental data themselves. It is known that the photoemission spectrum is a convolution of the single-electron Green’s function and a photoemission matrix element. It has been assumed that this matrix element is a constant, at least in a relevant range of parameters. Thus, relative intensities of different features of the spectrum were believed to be free of any influence extrinsic to the electron dynamics. However, it was shown recently that the matrix element has very non-trivial dependence on the photon energy and the binding energy of the photoelectrons [24]. In such a situation the significance of an intensity fit is substantially devaluated.

To conclude, we study the peak in the photoemission spectrum of BSCCO. It was shown that this peak is a consequence of the normal state pseudogap. We derived the most basic properties of the peak and demonstrated that they are in qualitative agreement with the experimental data available.

## VI. ACKNOWLEDGEMENTS

Author is most grateful to D. Basov, A.J. Millis and J.E. Hirsch for help and discussions.

## VII. APPENDIX

In this Appendix we will prove that under rather mild assumptions on  $G_n$  and  $\sigma^A$  the spectral function (11) satisfies (14). In our derivation we will assume that  $\mu \equiv 0$ . This limitation is not crucial.

An essential part of our proof is the analyticity of both  $G_n(\omega)$  and  $\sigma^A(\omega)$  for complex values of  $\omega$ ,  $\text{Im } \omega > 0$  (upper half-plane). First, we establish asymptotical behavior of  $G_n$  at large  $|\omega|$ . If  $|\omega| \gg W$  the details of the spectral function  $A(\omega)$  are irrelevant and it can be viewed as a delta function times  $2\pi$ . This means that at large  $|\omega|$ ,  $\text{Im } \omega > 0$

$$G_n(\omega) = \int_{-\infty}^{+\infty} \frac{d\omega'}{2\pi} \frac{A_n(\omega')}{\omega - \omega'} \simeq \frac{1}{\omega}. \quad (18)$$

We see, that due to the sum rule (14) the residue of  $G_n$  at infinity is exactly unity. Next, for any finite  $\omega^A$  the same reasoning can be applied to  $\sigma^A$  with the result:

$$\sigma^A(\omega) = \mathcal{O}(|\omega|^{-1}) \quad (19)$$

for large  $|\omega|$ . We do not try to determine the residue of  $\sigma^A$  at infinity since it is of no interest to us. The asymptotical behavior combined with the absence of any singularity in the upper half-plane of complex  $\omega$  implies that both  $G_n$  and  $\sigma^A$  are bounded:

$$|\sigma^A(\omega)| < C_\sigma, \quad (20)$$

$$|G_n(\omega)| < C_G. \quad (21)$$

where  $C_{\sigma,G}$  are some real positive constants. Now we are in position to prove that:

$$\text{Im} \int_{-\infty}^{+\infty} d\omega (G_s(\omega) - G_n(\omega)) = 0, \quad (22)$$

$$G_s(\omega) = \frac{G_n(\omega)}{1 - (\sigma^A(\omega))^2 (G_n(\omega))^2}, \quad (23)$$

provided that the product  $C_G C_\sigma < 1$ . This inequality guarantees that the denominator of  $G_s(\omega)$  never goes to zero. Therefore, the integrand of (22) has no singularities for  $\text{Im } \omega > 0$ . This means that we can transform the integration contour into a semi-circle in the upper half-plane. The integral over the semi-circle of infinite radius equals to the residue at infinity times  $(-\pi)$ . We already know that this residue is unity for  $G_n$ . It is also unity for  $G_s$ : at large  $|\omega|$  the denominator is non-singular and approaches 1, thus, the leading asymptotic behavior of  $G_s$  is the same as that of  $G_n$ . The residue of the integrand is zero which proves (22).

## REFERENCES

- [1] A. G. Loeser, Z.-X. Shen, M. C. Schabel, C. Kim, M. Zhang, A. Kapitulnik, P. Fournier, *Phys. Rev. B* **56**, 14185 (1997).
- [2] H.Ding, J.R. Engelbrecht, Z. Wang, J. C. Campuzano, S.-C. Wang, H.-B. Yang, R. Rogan, T. Takahashi, K. Kadowaki, D. G. Hinks, preprint cond-mat/0006143.
- [3] D.L.Feng, D.H. Lu, K.M. Shen, C. Kim, H. Eisaki, A. Damascelli, R. Yoshizaki, J.-i. Shimoyama, K. Kisho, G.D. Gu, S. Oh, A. Andrus, J. O'Donnell, J.N. Eckstein, and Z.-X. Shen, *Science* **280**, 277 (2000).
- [4] We use subscript 'n' ('s') to denote normal (superconducting) state quantities.
- [5] Gerald D. Mahan, "Many-Particle Physics", Plenum Press, 1990.
- [6] J.E. Hirsch, *Phys. Rev. B* **62**, 14487 (2000), J.E. Hirsch, *ibid.*, 14498 (2000).
- [7] M. Eschrig, M. R. Norman, *Phys. Rev. Lett.* **85**, 3261 (2000).
- [8] E.W. Carlson, D. Orgad, S.A. Kivelson, V.J. Emery, *Phys. Rev. B* **62**, 3422 (2000).
- [9] M.R. Norman, H. Ding, J.C. Campuzano, T. Takeuchi, M. Randeria, T. Yokoya, T. Takahashi, T. Mochiku, and K. Kadowaki, *Phys. Rev. Lett.* **79**, 3506 (1997).
- [10] M.R. Norman, H. Ding, *Phys. Rev. B* **57**, R11089 (1998).
- [11] For example, Ch. Renner, B. Revaz, J.-Y Genoud, K. Kadowaki, and Ø. Fischer, *Phys. Rev. Lett.* **80**, 149 (1998).
- [12] Sudip Chakravarty, Asle Sudbø, Philip W. Anderson, Steven Strong, *Science* **261**, 337 (1993).
- [13] O.K. Andersen, A.I. Liechtenstein, O. Jepsen and F. Paulsen, *J. Phys. Chem. Solids*, **56**, 1573 (1995).
- [14] T. Xiang, C. Panagopoulos, J.R. Cooper, *Int. J. Mod. Phys. B* **12**, 1007 (1998).
- [15] M. Randeria, Hong Ding, J-C. Campuzano, A. Bellman, G. Jennings, T. Yokoya, T. Takahashi, H. Katayama-Yoshida, T. Mochiku, and K. Kadowaki, *Phys. Rev. Lett.* **74**, 4951 (1995).
- [16] Unfortunately, the authors of [15] did not specify what is the frequency above which the symmetry of the spectrum is violated.
- [17] M. R. Norman, H. Ding, M. Randeria, J.C. Campuzano, T. Yokoya, T. Takeuchi, T. Takahashi, T. Mochiku, K. Kadowaki, P. Guptasarma & D.G. Hinks, *Nature* **392**, 157 (1998).
- [18] M. R. Norman, A. Kaminski, J. Mesot, J. C. Campuzano, *Phys. Rev. B* **63**, 140508 (2001).
- [19] If  $\sigma^A$  is a frequency-independent quantity then its imaginary part zero and, therefore,  $\text{Re}((\sigma^A)^2) = (\sigma^A)^2 > 0$ . Even if  $\sigma^A$  has some  $\omega$ -dependence  $\text{Re}(\sigma^A)^2$  is still positive in the range of interest provided that this dependence is a weak one.
- [20] D.S. Marshall, D.S. Dessau, A.G. Loeser, C-H. Park, A.Y. Matsuura, J.N. Eckstein, I. Bozovic, P. Fournier, A. Kapitulnik, W.E. Spicer, and Z.-X. Shen, *Phys. Rev. Lett.* **76**, 4841 (1996).
- [21] The author was unable to find any work done on the peak dispersion for the underdoped BSCCO. However, the data for the optimally doped and overdoped samples are available. For example, Ref. [9] shows that the dispersion curve of the peak for optimally doped sample is flat. Since most of the peak properties does not drastically change with doping we expect to have no dispersion on the underdoped side as well.

- [22] T. Sato, T. Kamiyama, Y. Naitoh, and T. Takahashi, I. Chong, T. Terashima, and M. Takano, *Phys. Rev. B* **63**, 132502-1 (2001).
- [23] Corson, J., Mallozzi, R., Orenstein, J., Eckstein, J.N. & Bozovic, I. *Nature* **398**, 221 (1999), A.J. Millis, *ibid.*, 193 (1999).
- [24] A. A. Kordyuk, S. V. Borisenko, T. K. Kim, K. Nenkov, M. Knupfer, M. S. Golden, J. Fink, H. Berger, R. Follath, cond-mat/0110379.

## FIGURES

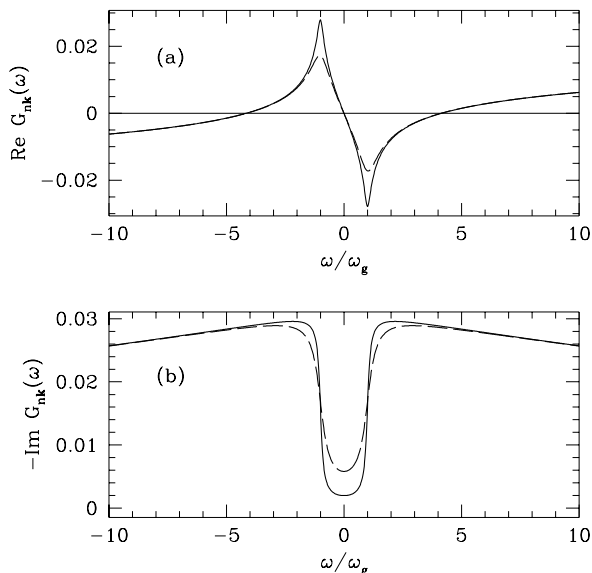


FIG. 1. Qualitative structure of the normal state Green's function for different values of  $\omega_e/\omega_g$ . The real part of  $G_n(\omega)$  (panel (a)) can be obtained by applying Kramers transformation to the imaginary part, panel (b). The solid line (dash-line) corresponds to  $\omega_e/\omega_g = 0.1$  ( $\omega_e/\omega_g = 0.3$ ).

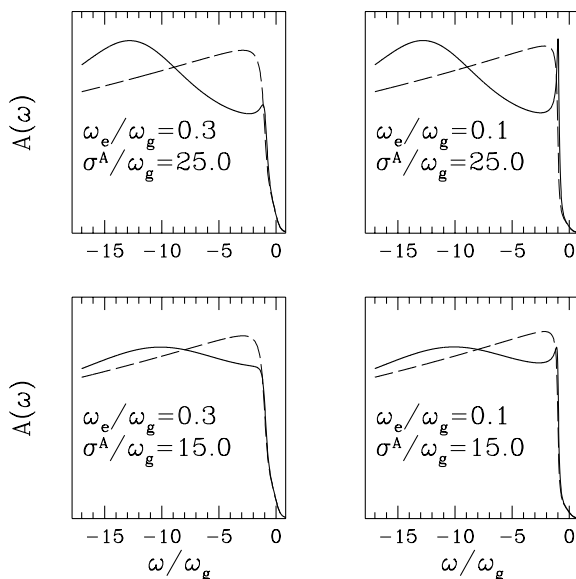


FIG. 2. Superconducting state spectral function ( $A_s(\omega)$  vs.  $\omega/\omega_g$ ) for  $W/\omega_g = 50$ ,  $\omega^A/\omega_g = 15$  and different values of  $\sigma^A/\omega_g$  and  $\omega_e/\omega_g$ . The left (right) column corresponds to  $\omega_e/\omega_g = 0.3$  ( $\omega_e/\omega_g = 0.1$ ). The top (bottom) row corresponds to  $\sigma^A/\omega_g = 25$  ( $\sigma^A/\omega_g = 15$ ). The normal state spectrum is given in a dash-line. The spectral functions are multiplied by the Fermi distribution function with  $T = 0.2\omega_g$ .

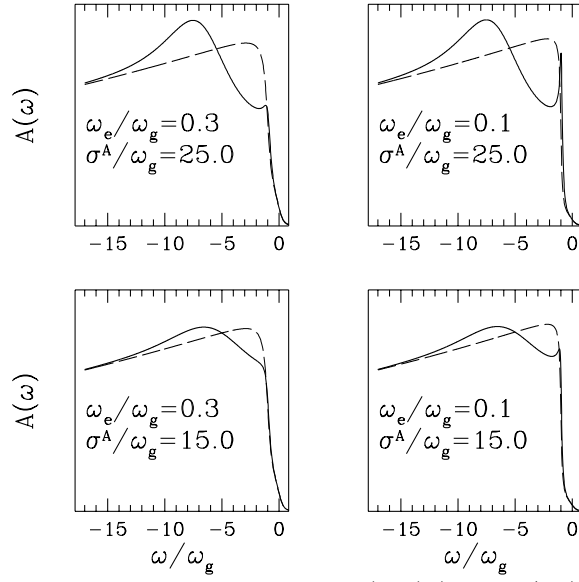


FIG. 3. Superconducting state spectral function ( $A_s(\omega)$  vs.  $\omega/\omega_g$ ) for  $W/\omega_g = 50$ ,  $\omega^A/\omega_g = 7$  and different values of  $\sigma^A/\omega_g$  and  $\omega_e/\omega_g$ . The left (right) column corresponds to  $\omega_e/\omega_g = 0.3$  ( $\omega_e/\omega_g = 0.1$ ). The top (bottom) row corresponds to  $\sigma^A/\omega_g = 25$  ( $\sigma^A/\omega_g = 15$ ). The normal state spectrum is given in a dash-line. The spectral functions are multiplied by the Fermi distribution function with  $T = 0.2\omega_g$ .

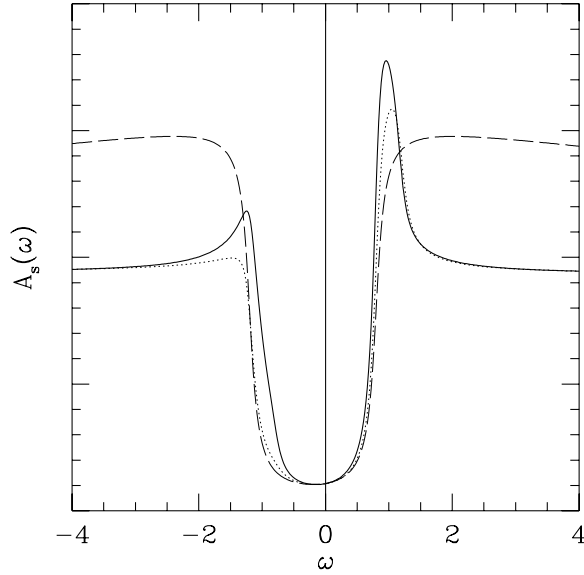


FIG. 4. The effect of weak particle-hole asymmetry on the superconducting spectral function. Normal state spectrum is shifted to the left by amount of  $\Delta\omega = 0.2\omega_g$ . The values of parameters are:  $W/\omega_g = 50$ ,  $\omega^A = \infty$ ,  $\omega_e/\omega_g = 0.1$ ,  $\sigma^A/\omega_g = 25$ . The normal state spectrum is given in a dash-line, the approximation (17) is plotted in a dotted line.